Low voltage operating $InGaZnO_4$ thin film transistors using high-*k* $MgO-Ba_{0.6}Sr_{0.4}TiO_3$ composite gate dielectric on plastic substrate

Dong Hun Kim,[1] Nam Gyu Cho,[1] Ho-Gi Kim,[1] Hyun-Suk Kim,[2] Jae-Min Hong,[3] and Il-Doo Kim[3,a)]

[1]*Department of Materials Science and Engineering, Korea Advanced Institute of Science and Technology, Daejeon 305-701, Republic of Korea*

[2]*Department of Materials Science and Engineering, Massachusetts Institute of Technology, Cambridge, Massachusetts 02139, USA*

[3]*Center for Energy Materials Research, Korea Institute of Science and Technology, P.O. Box 131 Cheongryang, Seoul 130-650, Republic of Korea*

(Received 8 May 2008; accepted 12 June 2008; published online 21 July 2008)

The authors report on the dielectric and leakage current properties of room temperature grown $MgO-Ba_{0.6}Sr_{0.4}TiO_3$ (MgO-BST) composite thin films to be utilized $InGaZnO_4$ thin films transistors (TFTs) fabricated on a polyethylene terephthalate (PET) substrate. The $InGaZnO_4$ TFTs with MgO-BST gate dielectrics exhibited low operation voltage of 4 V, high on/off current ratio of 4.13×10^6, and high field effect mobility of 10.86 $cm^2/V\,s$. These results verify that a room temperature grown MgO-BST gate dielectric is a good candidate for producing high performance $InGaZnO_4$ TFTs on plastic substrates. © *2008 American Institute of Physics*.
[DOI: 10.1063/1.2954014]

Recently, $InGaZnO_4$ films have been the focus of much interest as an active channel material for applications in transparent and flexible thin film transistors (TFTs).[1–3] In particular, $InGaZnO_4$ TFTs offer *n*-type semiconductor characteristics with a high mobility of more than 10 $cm^2/V\,s$ and a reasonably high on/off ratio.[4] Although $InGaZnO_4$ offers several attractive features, high voltage operation of $InGaZnO_4$ TFTs is still a major barrier for the realization of flexible, mobile, and battery-powered applications.[5] Therefore, it is important to use suitable gate dielectrics to drive low voltage operation of $InGaZnO_4$ TFTs fabricated on plastic substrates. In order to obtain a high on current at low applied bias, high permittivity gate dielectric or thickness reduction of the gate dielectric are required in order to increase the capacitive coupling of the gate electric field to the $InGaZnO_4$ layer. However, the requirement of maintaining a high capacity can no longer be accommodated by thickness reduction of gate dielectrics, particularly on plastic substrates, which have inherent high surface roughness and poor flatness. While there have been some early promising results for high-*k* gate dielectrics with $InGaZnO_4$ channel layer, i.e., Y_2O_3 (Refs. 1–4) and HfO_2,[6] room temperature grown high-*k* gate dielectrics are expected to suffer from poor leakage current characteristics at high voltage of >5 V, which is detrimental to $InGaZnO_4$ TFTs operation.

In this work, we investigate on structural and dielectric properties of a room temperature grown composite gate dielectric of $MgO-Ba_{0.6}Sr_{0.4}TiO_3$ (BST) for application in high performance $InGaZnO_4$ TFTs on plastic substrates. Although Kang *et al.* reported the role of 3% Mg acceptor doping in BST films, the phase was based on complete solid solution due to small amount of Mg doping.[7] There has been very little in-depth study of the dielectric behaviors of composite-gate dielectrics, i.e., excess MgO doped BST. Furthermore, no reports on excess MgO doped BST composite-gate dielectrics have provided clear evidence of the formation of a nanocrystalline phase, which would lead to improved leakage current characteristics, even when processed at room temperature. In this regard, the suitability of MgO-BST composite films as a gate dielectric for producing high performance $InGaZnO_4$ TFTs on a plastic substrate is discussed.

Disk-type undoped BST, (10, 20, and 30 mol % MgO)-BST, and $InGaZnO_4$ targets were prepared by a conventional mixed oxide method for pulsed laser deposition (PLD) and sputtering deposition. 300 nm thick undoped BST and 10 mol % MgO-BST ($MgO_{0.1}BST_{0.9}$), 20 mol % MgO-BST ($MgO_{0.2}BST_{0.8}$), and 30 mol % MgO-BST ($MgO_{0.3}BST_{0.7}$) thin films were deposited at room temperature using PLD and a sputtering method, respectively. For PLD deposition, a KrF excimer laser source ($\lambda=248$ nm) was employed with a repetition rate of 10 Hz and a fluence of 1–2 J/cm^2. For sputtering deposition, operating conditions of 80 W power, 60 mTorr working pressure, and a pure Ar gas atmosphere were used to deposit MgO-BST composite thin films.

For the dielectric and electrical measurements, a metal-insulator-metal (MIM) structure was formed on Pt coated Si substrates. Detailed measurement set-up is described elsewhere.[7] The microstructures were analyzed using a transmission electron microscope (TEM) (Tecnai 30 S-Twin) operated at 300 kV.

In order to investigate the suitability of MgO-BST composite thin films as a gate insulator, $InGaZnO_4$ TFTs were fabricated on a PET substrate. A 100 nm thick Cr gate electrode was deposited by dc magnetron sputtering using a shadow mask. Then, $MgO_{0.3}BST_{0.7}$ gate dielectrics and 40 nm thick $InGaZnO_4$ channel layers were deposited at room temperature by rf magnetron sputtering. Al source and drain were deposited by evaporation through shadow masks to obtain channel lengths of 50 μm and width of 2000 μm. The detailed TFTs experimental setup is described elsewhere.[7]

Figure 1 shows the dielectric constant-electric field characteristics of 300 nm thick BST and MgO-BST composite films deposited by PLD as a function of MgO content. The

a)Author to whom correspondence should be addressed. Electronic mail: idkim@kist.re.kr.

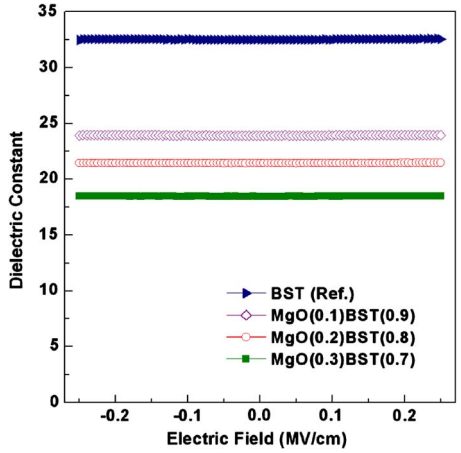

FIG. 1. (Color online) Dielectric constant-electric field characteristics of pure BST and MgO-BST composite thin films deposited by PLD.

pure BST thin films exhibited relatively high dielectric constants of 32.5. The effective relative dielectric constants of the 10, 20, and 30 mol % MgO-BST composite films are reduced to 24, 21, and 18, respectively due to the lower dielectric constant (~9.96) (Ref. 8) of MgO. The measured dielectric constants are similar to those evaluated from a series connection of MgO and BST as shown in the TEM image of Fig. 3(b). The dielectric constant can be calculated by the following equation:[9]

$$1/\varepsilon_{\text{MgO-BST}} = V_{\text{BST}}/\varepsilon_{\text{BST}} + V_{\text{MgO}}/\varepsilon_{\text{MgO}}, \quad (1)$$

where ε_{BST} and ε_{MgO} are the dielectric constants and V_{BST} and V_{MgO} are the volume fractions of BST and MgO. The dielectric constants of $MgO_{0.1}BST_{0.9}$, $MgO_{0.2}BST_{0.8}$, and $MgO_{0.3}BST_{0.7}$ films evaluated by Eq. (1) are 25.7, 21.3, and 18.4, respectively. The values of the calculated dielectric constants correspond relatively well with the measured dielectric constant values. Although higher MgO content results in a lower dielectric constant of the MgO-BST composite films, the dielectric constant (~18) of $MgO_{0.3}BST_{0.7}$ thin film remains high enough to achieve low voltage operation of less than 10 V in $InGaZnO_4$ TFTs.

Figure 2 illustrates the current density-electric field characteristics of PLD grown BST and MgO-BST composite thin films measured in a MIM configuration. The magnitude of the leakage current density at a given electric field indicates that there is obvious dependence on the variation of MgO

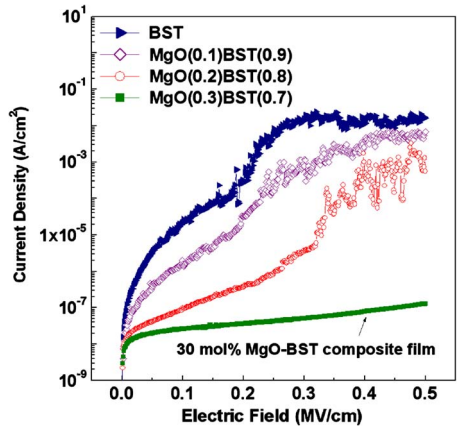

FIG. 2. (Color online) Leakage current characteristics of pure BST and MgO-BST composite thin films deposited by PLD.

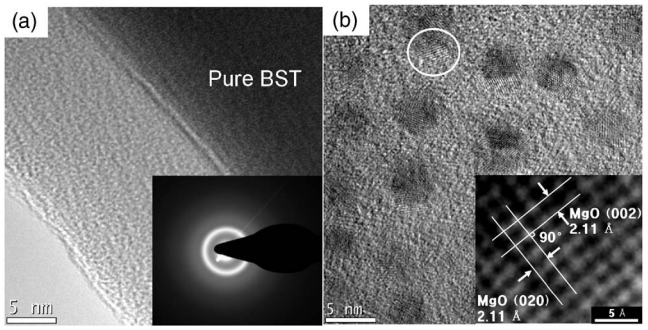

FIG. 3. (a) HR-TEM image of pure BST thin films. The inset exhibits a selected area diffraction pattern of the BST thin films. (b) HR-TEM image of MgO-BST composite thin films. The inset shows the lattice fringe of MgO nanoparticles.

content. With increasing MgO content, the leakage current markedly decreased. A remarkable reduction in the leakage current density could be achieved with a $MgO_{0.3}BST_{0.7}$ ratio. MgO, i.e., a wide bang gap insulator, is expected to reduce the leakage current density due to its low dielectric constant and low-loss value. As shown in Fig. 2, the measured leakage current density of the $MgO_{0.3}BST_{0.7}$ composite film remained on the order of $\sim 2\times 10^{-8}$ A/cm^2 even up to an applied electric field of 0.5 MV/cm, thus demonstrating significant improvement in leakage current characteristics. On the other hand, the undoped BST thin film showed poor leakage current properties, i.e., low breakdown strength at 0.3 MV/cm, as shown in Fig. 2. Based on the above results, optimum device operation could be anticipated with the use of $MgO_{0.3}BST_{0.7}$ composite films, which have a reasonably high dielectric constant (~18) and offer enhanced leakage current characteristics. Therefore, we have fixed the composition of the composite gate insulator, i.e., $MgO_{0.3}BST_{0.7}$, and optimized the process parameters using sputtering to provide large area device performance for the fabricated $InGaZnO_4$ TFTs. The dielectric constant of $MgO_{0.3}BST_{0.7}$ thin films deposited by sputtering was reasonably high at 20. This is comparable with that (18) of PLD grown $MgO_{0.3}BST_{0.7}$ thin films. In particular, markedly improved leakage current characteristics were observed in room temperature grown $MgO_{0.3}BST_{0.7}$ thin films deposited by sputtering. The measured leakage current density remained on the order of $\sim 1\times 10^{-8}$ A/cm^2, even up to an applied electric field of 2 MV/cm (not shown). As shown in Fig. 2, the leakage current of the $MgO_{0.3}BST_{0.7}$ thin films is significantly reduced by several orders of magnitude as compared to that of pure BST thin films. This may be attributed to the existence of excess MgO, which would disperse randomly in the amorphous BST matrix. Thus, MgO plays an important role in blocking charge transport in the BST matrix.

In order to confirm this, we conducted a TEM analysis. Figure 3(a) shows a high resolution TEM (HR-TEM) image of pure BST thin film. The inset exhibits a selected area diffraction pattern of a BST thin film. It is verified that the pure BST films have an amorphous structure. On the other hand, the HR-TEM image of the $MgO_{0.3}BST_{0.7}$ composite film shows a locally dispersed nanocrystalline phase in an amorphous matrix, as shown in Fig. 3(b). The diffraction ring pattern confirms that the crystalline phase was MgO. The *d*-spacings calculated from each rings are 2.46, 2.12, 1.48, and 1.25 Å and they are well matched with (100), (200), (220), and (311) of MgO, respectively, as reported in

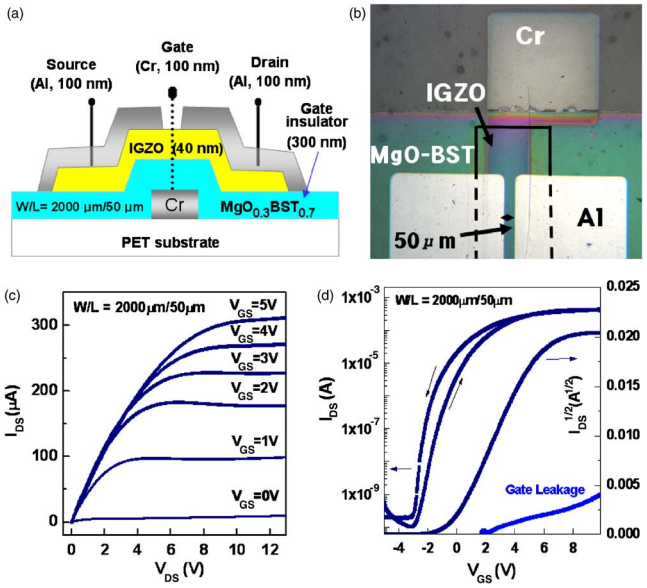

FIG. 4. (Color online) (a) A schematic diagram of an $InGaZnO_4$ TFT with a $MgO_{0.3}BST_{0.7}$ gate dielectric on a PET substrate. (b) Top view of the $InGaZnO_4$ TFT fabricated on a PET substrate taken by optical microscopy. (c) Output characteristics: drain-to-source current (I_{DS}) as a function of the drain-to-source voltage (V_{DS}) at various gate-to-source voltages (V_{GS}), [a channel length (L) of 50 μm and a channel width (W) of 2000 μm]. (d) Transfer characteristics: drain-to-source current (I_{DS}) as a function of the gate-to-source voltage (V_{GS}). V_{GS} was swept from −5 to 10 V at V_{DS} of 4 V.

Ref. 10. The inset of Fig. 3(b) presents a magnified view of the local nanocrystalline phase of MgO. Two planes exhibited perpendicular alignment. The interplanar spacing is about 2.11 Å, which corresponds to the (200) planes of MgO. Therefore, the uniform distribution of MgO nanoparticles could suppress leakage current flow in the BST matrix due to their excellent insulating characteristics. This means that a potential barrier could be built at the localized MgO/BST interfaces due to the different band gap between MgO (~7 eV) (Ref. 11) and BST (~4.3 eV).[12] The good leakage current characteristics of $MgO_{0.3}BST_{0.7}$ gate dielectrics would be beneficial to the $InGaZnO_4$ TFTs performance. To verify this, we fabricated bottom gate and top contact $InGaZnO_4$ TFTs using room temperature grown $MgO_{0.3}BST_{0.7}$ gate dielectrics on PET substrates. A schematic diagram and photoimage of the TFTs are presented in Figs. 4(a) and 4(b), respectively.

Figure 4(c) shows the drain-to-source current (I_{DS}) as a function of the drain-to-source voltage (V_{DS}) at various gate-to-source voltages (V_{GS}) of $InGaZnO_4$ TFTs with $MgO_{0.3}BST_{0.7}$ dielectrics. The $InGaZnO_4$ TFTs exhibit n-channel behavior operating in accumulation mode, since electrons are generated by the positive gate voltage (V_{GS}). The TFTs do not conduct at a gate voltage of 0 V. In particular, a superior gate-modulated characteristic with good drain-to-source current saturation was observed, as shown in Fig. 4(c). I_{DS} increased with an increase of V_{DS} at low drain voltage and showed saturation behavior at moderate drain voltage due to pinch off of the accumulation layer in the $InGaZnO_4$ channel layer. The high capacitance of the $MgO_{0.3}BST_{0.7}$ gate dielectrics resulted in low voltage operation of less than 4 V. The TFTs with $MgO_{0.3}BST_{0.7}$ gate dielectric exhibited high on current of 300 μA at V_{GS}=5 V.

Figure 4(d) shows the transfer characteristics of $InGaZnO_4$ TFTs with $MgO_{0.3}BST_{0.7}$ gate dielectrics. The gate voltage was swept from −5 to 10 V at a fixed I_{DS} of 4 V. Under these conditions, I_{DS} can be influenced by the field effect mobility (μ_{FE}), the gate dielectric capacitance (C_i), the aspect ratio of the device (W/L), the gate voltage (V_G), and the threshold voltage (V_{th}), as shown below.

$$\sqrt{I_{DS}} = \sqrt{\frac{W}{2L}C_i\mu(V_{GS} - V_{th})}. \quad (2)$$

As indicated in Eq. (2), the saturation mobility can be derived from the slope of the $(I_{DS})^{1/2}$ versus V_{GS} curve while the threshold voltage (V_{th}) of the device can be estimated by extrapolation of the linear portion of the curve to zero drain current. As shown in Fig. 4(d), the on current and off current of the $InGaZnO_4$ TFTs were measured as 4.18×10^{-4} and 1.01×10^{-10} A, respectively, giving an on/off current ratio of 4.13×10^6. The measured V_{th} and μ_{FE} were −0.34 V and 10.86 $cm^2/V\,s$, respectively. The subthreshold swing (SS) was 0.46 V/decade. The SS value is slightly larger than that of $InGaZnO_4$ TFTs using SiN_x dielectric (~0.2 V/decade) deposited at 300 °C and annealed at 350 °C.[13,14] This result may be attributed to the interface trap between semiconductor and high-k gate dielectric. We could expect further enhancement of SS value by interface improvement.

In summary, we investigated the role of excess MgO in a BST matrix as a gate dielectric. A remarkable reduction in leakage current density could be achieved in $MgO_{0.3}BST_{0.7}$ composite thin films due to the suppression of charge carrier transport. $InGaZnO_4$ TFTs with $MgO_{0.3}BST_{0.7}$ composite gate dielectrics showed low voltage operation of 4 V due to the high dielectric constant of $MgO_{0.3}BST_{0.7}$. The TFTs showed high field effect mobility of 10.86 $cm^2/V\,s$ and a moderate on/off ratio of 4.13×10^6. The subthreshold swing and threshold voltage were 0.46 V/decade and −0.34 V, respectively. These results demonstrate the potential use of room temperature grown $MgO_{0.3}BST_{0.7}$ composite thin films as a promising gate dielectric for producing $InGaZnO_4$ TFTs fabricated on plastic substrates.

This work was supported in part by Seoul R&BD Program under Contract No. 2G07270.

[1]H. Hosono, J. Non-Cryst. Solids **352**, 851 (2006).
[2]K. Nomura, A. Takagi, T. Kamiya, H. Ohta, M. Hirano, and H. Hosono, Jpn. J. Appl. Phys., Part 1 **45**, 4303 (2006).
[3]H. Kumomi, K. Nomura, T. Kamiya, and H. Hosono, Thin Solid Films **516**, 151 (2008).
[4]H. Yabuta, M. Sano, K. Abe, T. Aiba, K. Nomura, T. Kamiya, and H. Hosono, Appl. Phys. Lett. **89**, 112123 (2006).
[5]A. Suresh, P. Wellenius, A. Dhawan, and J. Muth, Appl. Phys. Lett. **90**, 123512 (2007).
[6]K. Nomura, H. Ohta, K. Ueda, T. Kamiya, M. Hirano, and H. Hosono, Science **300**, 1269 (2003).
[7]K. Kang, M.-H. Lim, H.-G. Kim, I.-D. Kim, and J.-M. Hong, Appl. Phys. Lett. **90**, 043502 (2007).
[8]H. W. Choi, S. Y. Kim, W.-K. Kim, and J.-L. Lee, Appl. Phys. Lett. **87**, 082102 (2005).
[9]M. Jain, S. B. Majumder, R. S. Katiyar, and A. S. Bhalla, Mater. Lett. **57**, 4232 (2003).
[10]JCPDS Card No. 65-0476.
[11]T. Uhrmann, T. Dimopoulis, H. Bruckl, V. K. Lazarov, A. Kohn, U. Paschen, S. Weyers, L. Bar, and M. Ruhrig, J. Appl. Phys. **103**, 063709 (2008).
[12]T. Kikkawa, N. Fujiwara, H. Yamada, S. Miyazaki, F. Nishiyama, and M. Hirose, Appl. Phys. Lett. **81**, 2821 (2002).
[13]D. Kang, H. Lim, C. Kim, I. Song, J. Park, Y. Park, and J. Chung, Appl. Phys. Lett. **90**, 192101 (2007).
[14]J. H. Jeong, H. W. Yang, J.-S. Park, J. K. Jeong, Y.-G. Mo, H. D. Kim, J. Song, and C. S. Hwang, Electrochem. Solid-State Lett. **11**, H157 (2008).